

Dynamical generation of the scalar $f_0(500)$, $f_0(980)$ and $K_0^*(700)$ resonances in the $D_s^+ \rightarrow K^+\pi^+\pi^-$ reaction

L. R. Dai^{a,*} and E. Oset^b

^a*School of Science, Huzhou University, Huzhou 313000, Zhejiang, China*

^b*Departamento de Física Teórica and IFIC, Centro Mixto Universidad de Valencia-CSIC Institutos de Investigación de Paterna, Aptdo.22085, 46071 Valencia, Spain*

E-mail: dailianrong@zjhu.edu.cn

In this talk, we present the recent work for the Cabibbo-suppressed $D_s^+ \rightarrow K^+\pi^+\pi^-$ decay, which was recently measured by the BESIII collaboration. We investigate the dynamical generation of the scalar $f_0(500)$, $f_0(980)$ and $K_0^*(700)$ resonances in which three mass distributions of pairs of mesons in this reaction are shown. The largest contributions to the process come from the $D_s^+ \rightarrow K^+\rho^0$ and $D_s^+ \rightarrow K^{*0}\pi^+$ decay modes, but the $D_s^+ \rightarrow K_0^*(1430)\pi^+$ and $D_s^+ \rightarrow K^+f_0(1370)$ modes also play a moderate role and all of them are introduced empirically. Instead, the contribution of the $f_0(500)$, $f_0(980)$ and $K_0^*(700)$ resonances is introduced dynamically by looking at the decay modes at the quark level, hadronizing $q\bar{q}$ pairs to give two mesons, and allowing these mesons to interact, for which we follow the chiral unitary approach, to finally produce the $K^+\pi^+\pi^-$ final state. While the general features of the mass distributions are fairly obtained, we pay special attention to the specific effects created by the light scalar resonances, which are visible in the low mass region of the $\pi^+\pi^-$ ($f_0(500)$) and $K^+\pi^-$ ($K_0^*(700)$) mass distributions and a narrow peak for $\pi^+\pi^-$ distribution corresponding to $f_0(980)$ excitation. The contribution of these three resonances is generated by only one parameter. We see the agreement found in these regions as further support for the nature of the light scalar states as dynamically generated from the interaction of pseudoscalar mesons.

10th International Conference on Quarks and Nuclear Physics (QNP2024)

8-12 July, 2024

Barcelona, Spain

*Speaker

1. Introduction

The $D_s \rightarrow K^+\pi^+\pi^-$ decay has been measured by BESIII collaboration with better statistics [1]. We are interested in this reaction, because it is a Cabibbo-suppressed decay and no theoretical work on this particular channel is available to the best of our knowledge. That is why we wish to address this problem [2].

In the $D_s \rightarrow K^+\pi^+\pi^-$ decay, in addition to the dominant mode $D_s^+ \rightarrow K^+\rho, \rho \rightarrow \pi^+\pi^-$ and $D_s^+ \rightarrow K^*(892)^0\pi^+, K^*(892)^0 \rightarrow K^+\pi^-$, the experiment finds traces of the $f_0(500)$, $f_0(980)$ and $f_0(1370)$ resonances. The aim in the present work: 1) we relate the production of the $f_0(500)$, $f_0(980)$ and $K_0^*(700)$ scalar resonances by the chiral unitary approach [3]. 2) One looks at the main production modes at the quark level based on external emission and internal emission [4], and then proceeds with the hadronization of the $q\bar{q}$ pairs in order to produce the coupled channels needed to generate these resonances. 3) The nice thing is that we can correlate the production of these resonances by means of only one parameter. 4) This procedure is different from the experimental analyses where the production of each of these resonances is parametrized and fitted to the data. It should be stressed that our approach is very restrictive, and the eventual agreement with the data comes to support the picture of these resonances as being dynamically generated from the interaction of pseudoscalar mesons.

2. Formalism and Results

At first, at the quark level, we look at the different topologies that can contribute to this Cabibbo-suppressed process.

Figure 1 produces a π^+ and K^{*0} with external emission, and $K^{*0} \rightarrow K^+\pi^-$, this is one important mode observed in the BESIII experiment [1]. Figure 2 produces a ρ^0 meson and a K^+ , and the $\rho^0 \rightarrow \pi^+\pi^-$, again one important mode observed in the BESIII experiment [1].

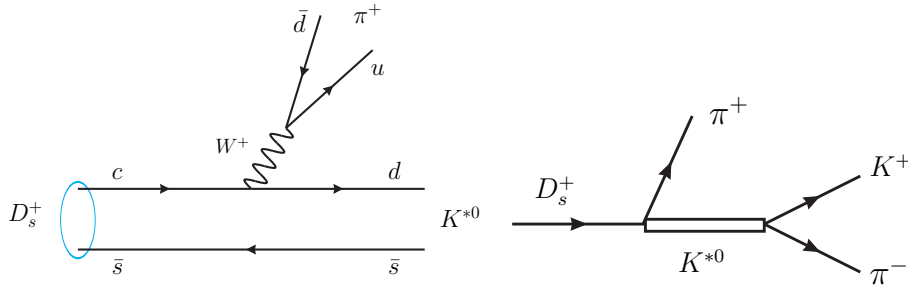


Figure 1: Mechanism for production of $D_s^+ \rightarrow \pi^+K^{*0}$ with external emission and $K^{*0} \rightarrow K^+\pi^-$.

Next we look at the production of three pseudoscalar mesons. This is accomplished by hadronizing a $q\bar{q}$ component into two pseudoscalar mesons. It is seen that in Figure 3, a K^+ is produced in external emission and the $s\bar{s}$ component is hadronized into two pseudoscalars. The Cabibbo-suppressed $W\bar{s}u$ vertex appears in the upper part; in Figure 4 again with external emission, a π^+ is produced and the $d\bar{s}$ component is hadronized into two pseudoscalars. The Cabibbo-suppressed $Wc\bar{d}$ vertex appears in the lower part. Both vertices imply the same reduction factor of $\sin\theta_c$. In Figure 5 the mechanism proceeds via internal emission, a K^+ is produced and the $s\bar{s}$ component is

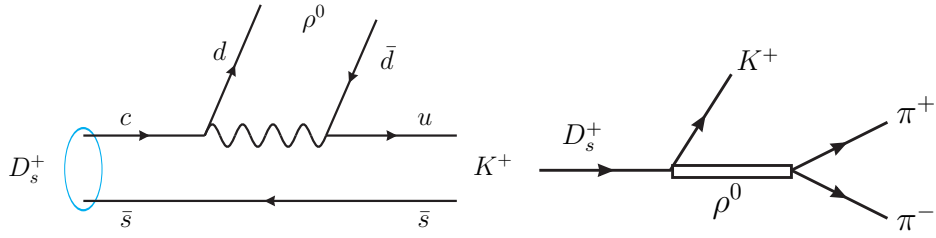


Figure 2: Mechanism for $D_s^+ \rightarrow \rho K^+$ with internal emission and $\rho^0 \rightarrow \pi^+\pi^-$.

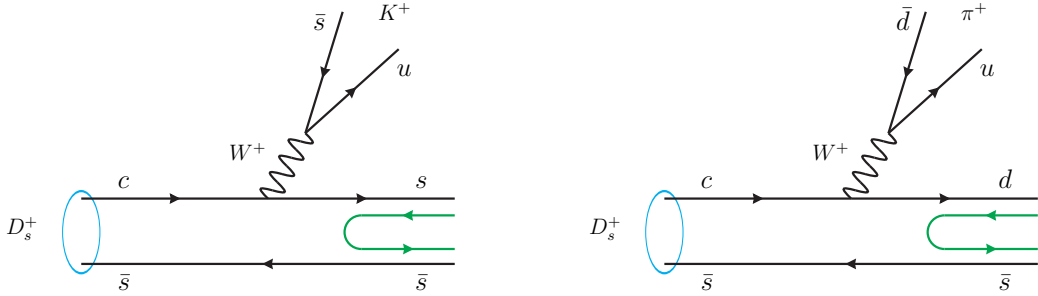


Figure 3: $D_s^+ \rightarrow K^+ s\bar{s}$ with external emission and $s\bar{s}$ hadronization.

Figure 4: $D_s^+ \rightarrow \pi^+ d\bar{s}$ with external emission and $d\bar{s}$ hadronization.

hadronized into two pseudoscalars. In Figure 6 again with internal emission a K^+ is produced and the $d\bar{d}$ component is hadronized into two pseudoscalars. Both vertices imply the same reduction factor of $\sin \theta_c$. We can see that in Figure 6 we already obtain $K^+\pi^-\pi^+$ at the tree level, but we also

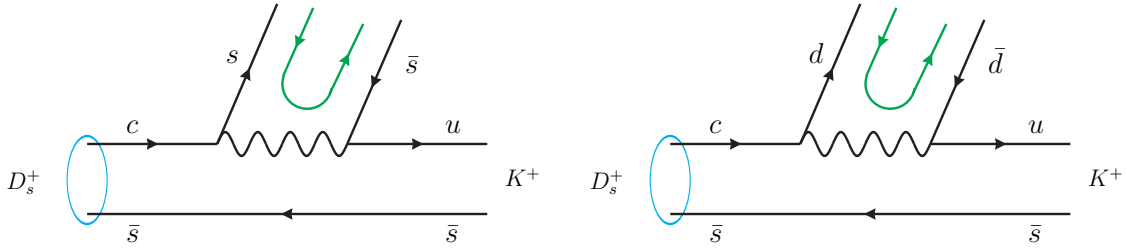


Figure 5: $D_s^+ \rightarrow K^+ s\bar{s}$ with internal emission followed by $s\bar{s}$ hadronization.

Figure 6: $D_s^+ \rightarrow K^+ d\bar{d}$ with internal emission and $d\bar{d}$ hadronization.

get other intermediate states that upon rescattering lead to the same state, as depicted in Figure 7.

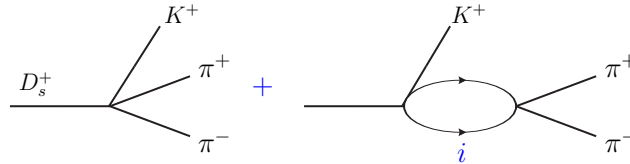


Figure 7: Direct $K^+\pi^-\pi^+$ production (tree level) and production through intermediate states, $i = \pi^+\pi^-$, $\pi^0\pi^0$, $\eta\eta$, $\pi^0\eta$, K^+K^- , $K^0\bar{K}^0$ in general.

We can write the production matrix for each mechanism, for instance,

$$t^{(3)} = \sum_i \alpha h W_i G_i t_{i, \pi^+\pi^-} \quad (1)$$

which corresponds to Figure 3, the h factor accounting for the mechanism of hadronization, G_i are the meson-meson loop functions and $t_{i, \pi^+\pi^-}$ the scattering matrices for transitions of the state i in the loop to the $\pi^+\pi^-$ final state. The intermediate states: $i = K^+K^-, K^0\bar{K}^0, \eta\eta$, and the weights $W_{K^+K^-} = 1, W_{K^0\bar{K}^0} = 1, W_{\eta\eta} = \frac{2}{3}\frac{1}{\sqrt{2}}$.

For Figure. 4 we obtain

$$t^{(4)} = \alpha h \left\{ 1 + \sum_i \tilde{W}_i G_i(M_{\text{inv}}, \pi^-K^+) t_{i, \pi^-K^+}(M_{\text{inv}}, \pi^-K^+) \right\} \quad (2)$$

with $i = \pi^-K^+, \pi^0K^0$ and weights $\tilde{W}_{\pi^-K^+} = 1, \tilde{W}_{\pi^0K^0} = -\frac{1}{\sqrt{2}}$. For Figures 5 and 6 we obtain

$$t^{(5+6)} = \gamma h \left\{ 1 + \sum_i W'_i G_i(M_{\text{inv}}, \pi\pi) t_{i, \pi^+\pi^-}(M_{\text{inv}}, \pi\pi) \right\} \quad (3)$$

$W'_{\pi^+\pi^-} = 1, W'_{\pi^0\pi^0} = \frac{1}{\sqrt{2}}, W'_{K^+K^-} = 1, W'_{K^0\bar{K}^0} = 2, W'_{\eta\eta} = \frac{4}{3}\frac{1}{\sqrt{2}}, W'_{\pi^0\eta} = -\sqrt{\frac{2}{3}}$

We look to the mechanisms in Figures 1 and 2 for K^{*0} and ρ^0 production, respectively, including their corresponding decays. In both cases, we have $K^+\pi^+\pi^-$ in the final state. We use the standard Lagrangian to obtain the $K^{*0} \rightarrow K^+\pi^-, \rho^0 \rightarrow \pi^+\pi^-$ vertices. The amplitudes in terms of the invariant masses s_{12}, s_{13}, s_{23} for the particles in the order $\pi^-(1), \pi^+(2), K^+(3)$ can be written as

$$t^{(1)} = \alpha g \frac{1}{s_{13} - m_{K^*}^2 + i m_{K^*} \Gamma_{K^*}} \left\{ -s_{23} + s_{12} + \frac{(m_{K^+}^2 - m_{\pi^-}^2)(m_{D_s}^2 - m_{\pi^+}^2)}{m_{K^*}^2} \right\}, \quad (4)$$

where $s_{13} = (P_{\pi^-} + P_{K^+})^2, s_{12} = (P_{\pi^-} + P_{\pi^+})^2, s_{23} = (P_{\pi^+} + P_{K^+})^2$.

$$t^{(2)} = \gamma g \sqrt{2} \frac{1}{s_{12} - m_{\rho}^2 + i m_{\rho} \Gamma_{\rho}} \{-s_{13} + s_{23}\},$$

$$s_{12} + s_{23} + s_{13} = m_{D_s}^2 + m_{K^+}^2 + m_{\pi^+}^2 + m_{\pi^-}^2. \quad (5)$$

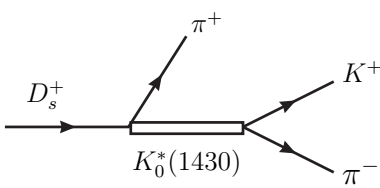


Figure 8: Mechanism for $D_s^+ \rightarrow \pi^+ K_0^*(1430)$ and then $K_0^*(1430) \rightarrow K^+\pi^-$

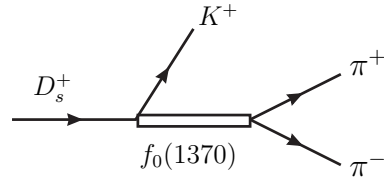


Figure 9: Mechanism for $D_s^+ \rightarrow K^+ f_0(1370)$ and then $f_0(1370) \rightarrow \pi^+\pi^-$

Following the analysis of the experimental work, we also allow the contribution of two scalar resonances, the $f_0(1370)$ and $K_0^*(1430)$ [1]. For Figure 7 and 8, we have the amplitudes

$$t^{(7)} = \beta \frac{m_{D_s}^2}{s_{13} - m_{K_0^*(1430)}^2 + i m_{K_0^*(1430)} \Gamma_{K_0^*(1430)}}, t^{(8)} = \delta \frac{m_{D_s}^2}{s_{12} - m_{f_0(1370)}^2 + i m_{f_0(1370)} \Gamma_{f_0(1370)}}. \quad (6)$$

These two resonances are obtained, from vector-vector interaction in the chiral unitary approach with less precision of 150 – 200 MeV mass difference [5, 6], hence we introduce them empirically as free parameters.

The sum of all amplitudes

$$t = t^{(1)} + t^{(2)} + t^{(3)} + t^{(4)} + t^{(5+6)} + t^{(7)} + t^{(8)}. \quad (7)$$

and finally we obtain the mass distribution

$$\frac{d^2\Gamma}{dm_{12}^2 dm_{23}^2} = \frac{1}{(2\pi)^3} \frac{1}{32M_{D_s}^3} |t|^2, \quad (8)$$

where $m_{12}^2 = s_{12}$ for $\pi^+\pi^-$ and $m_{23}^2 = s_{23}$ for π^+K^+ . We integrate Eq. (8) over s_{23} with the limits of the PDG and obtain $d\Gamma/dm_{12}^2$. By cyclical permutation of the indices we easily obtain $d\Gamma/dm_{13}^2$ and $d\Gamma/dm_{23}^2$.

By conducting a best fit to the experimental data of three invariant mass distributions [1], we obtain the following parameters $\alpha = 14.67 \pm 1.28$, $h = 6.86 \pm 2.57$, $\gamma = 10.75 \pm 2.31$, $\beta = -33.23 \pm 24.85$, $\delta = -58.84 \pm 31.27$ and the final results are given in Figure. 10. We can see that the agreement with the data is relatively fair and the K^{*0} , ρ^0 peaks are prominent in the reaction. The errors in the β and γ parameters are larger, indicating a minor role of the $K_0^*(1430)$ and $f_0(1370)$ resonances. The $K_0^*(1430)$ contribution is observed as a soft peak in the $K^+\pi^-$ mass spectrum around 1400 MeV. The $f_0(1370)$, which has a very large width, shows up in the $\pi^+\pi^-$ spectrum around 1200 - 1400 MeV.

In the low energy part of the $\pi^+\pi^-$ mass spectrum, we can see the contributions of $f_0(500)$, the sharp peak of $f_0(980)$; In the low energy part of the $K^+\pi^-$ mass spectrum, we can see the contribution of $K_0^*(700)$. We stress that we only have a unique parameter h for all contributions from these three resonances. The fair reproduction of the spectra supports that these contributions are indeed correlated. Our mechanism produces a fair reproduction in these three $\pi^+\pi^-$, $K^+\pi^+$, $K^+\pi^-$ mass distributions.

3. Conclusions

We investigate the dynamical generation of the scalar $f_0(500)$, $f_0(980)$ and $K_0^*(700)$ resonances in which three mass distributions of pairs of mesons in this reaction are shown. The general features of the mass distributions are fairly obtained, and we pay special attention to the low mass region of the $\pi^+\pi^-$ ($f_0(500)$) and $K^+\pi^-$ ($K_0^*(700)$) mass distributions and a narrow peak for $\pi^+\pi^-$ distribution corresponding to $f_0(980)$ excitation. The contribution of these three resonances is generated by only one parameter. The agreement with experiments would support the nature of the light scalar states as dynamically generated from the interaction of pseudoscalar mesons.

Acknowledgments

This work is supported by the National Natural Science Foundation of China under Grants Nos. 12175066 and 11975009.

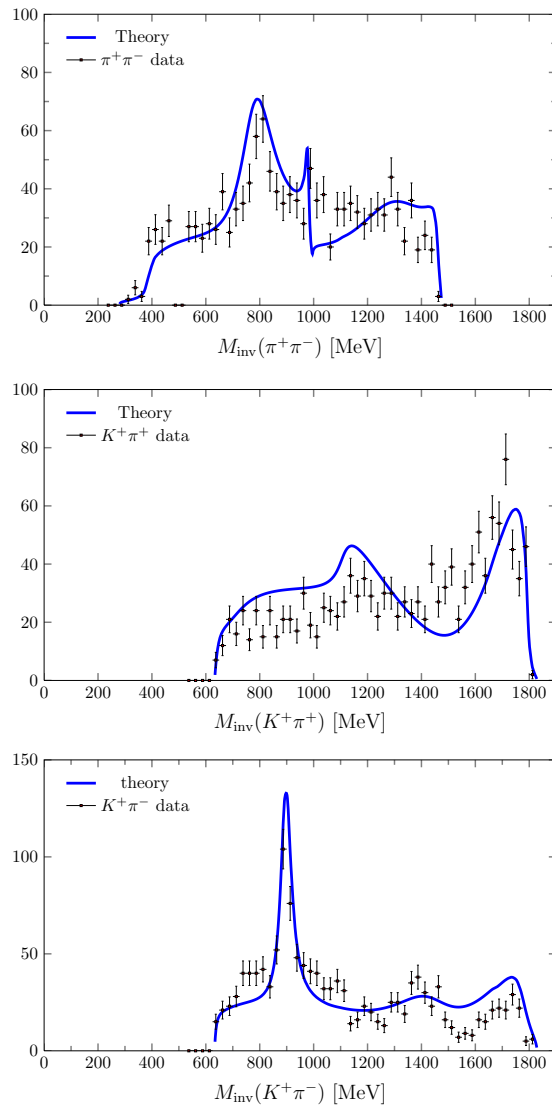


Figure 10: Invariant mass distributions about $\pi^+\pi^-$, $K^+\pi^+$ and $K^+\pi^-$.

References

- [1] M. Ablikim et al. (BESIII Collaboration), *J. High Energy Phys.* **08** (2022) 196
- [2] L. R. Dai, E. Oset, *Phys. Rev. D* **109** (2024) 054008
- [3] J. A. Oller, E. Oset, and A. Ramos, *Prog. Part. Nucl. Phys.* **45** (2000) 157
- [4] L. L. Chau, *Phys. Rept.* **95** (1983) 1
- [5] R. Molina, D. Nicmorus, and E. Oset, *Phys. Rev. D* **78** (2008) 114018
- [6] L. S. Geng and E. Oset, *Phys. Rev. D* **79** (2009) 074009